JOURNAL OF NANO- AND ELECTRONIC PHYSICS
Vol. **5** No 4, 04013(4pp) (2013)

ЖУРНАЛ НАНО- ТА ЕЛЕКТРОННОЇ ФІЗИКИ
Том **5** № 4, 04013(4cc) (2013)

Magnetic Properties of $A^{II}B^{IV}C^{V}_2$ Compounds Doped with Mn

A.V. Kochura[1,2,*], S.V. Ivanenko[1], A. Lashkul[2], E.P. Kochura[1], S.F. Marenkin[3], I.V. Fedorchenko[3], A.P. Kuzmenko[1], E. Lahderanta[2],

[1] *Southwest State University, 94, 50 Let Oktjabrja Str., 305040 Kursk, Russia*
[2] *Laboratory of Physics, Lappeenranta University of Technology, PO Box 20, FIN-53851 Lappeenranta, Finland*
[3] *Institute of General and Inorganic Chemistry of Russian Academy of Sciences, 31, Leninskii Pr., 119991 Moscow, Russia*

(Received 20 September 2013; published online 10 December 2013)

Mn-doped $A^{II}B^{IV}C^{V}_2$ semiconductors bulk crystals were grown by direct melting of base components with fast cooling. Structural and magnetic properties of samples were investigated. Analysis of the temperature dependence of the magnetization reveals three types of magnetic species: the substitutional Mn ions making Mn complexes (especially dimers), the MnAs micro- and nanosize precepitates.

Keywords: Spintronic materials, Chalcopyrite semiconductors, Magnetization, Nanoclusters.

PACS numbers: 81.05.Cy, 75.50.Tt, 75.60.Ej

1. INTRODUCTION

Today a new branch of electronics, called spintronics, is developing rapidly. In spintronic devices is used materials, which allow to control the spin and charge degrees of freedom [1]. This is their advantage over traditional electronic devices. One of main difficulties of spin components is the absence of materials, which can operate in temperatures similar to traditional electronics. Using of Fe, Co and Ni is not effective, because of they have different crystal structure and electronic properties with semiconductors. Therefore in the present time the search is carried out in different directions, among which d-elements doping of materials, which are used in modern electronics (Si, Ge, III-As and others) [1]. One of most perspective materials for spintronic applications is Mn-doped GaAs [2]. In the past decade many important spintronic applications have been realized based on this material, including electrical-field control of the Curie temperature and magnetization, spin injection into non-magnetic semiconductors, tunneling magnetoresistance and electric current induced magnetization reversal [3]. However, the highest obtained Curie temperatures for GaMnAs films ($T_C \approx 185$ K) [4] and for heavily Mn-doped (Ga,Mn)As nanowires ($T_C \sim 200$ K) [5] are lower than the room temperature. Ternary chalcopyrite semiconductors of the $A^{II}B^{IV}C^{V}_2$ system are considered as structural and electronic counterparts of III-As compounds [6]. $CdSnAs_2$, $ZnGeAs_2$, $CdSnP_2$, and $ZnGeP_2$ are "direct" analogues of the InAs, GaAs, InP, and GaP, respectively. They have better solubility of d-elements and can easily accept a high concentration of Mn atoms, which is a natural property of chalcopyrites used as two-cation semiconductor [7].

Theoretical estimates of magnetic order in Mn-doped $A^{II}B^{IV}C^{V}_2$ compounds showed that, only 19 of them can retain ferromagnetic properties and only with higher Mn content [8]. In $A^{II}B^{IV}C^{V}_2$ compounds ferromagnetism above room temperature was experimentally observed first in single-crystal $Cd_{1-x}Mn_xGeP_2$ films [9]. Now 8 compounds with high temperature ferromagnetic ordering are known among Mn-doped $A^{II}B^{IV}C^{V}_2$ semiconductors [10]. For such materials the highest $T_C \sim 367$ K has been observed for $ZnGeAs_2$, doped with Mn [11].

It is stimulated interest to elaborate growing process of the Mn-doped $A^{II}B^{IV}C^{V}_2$ semiconductors, including $Cd_{1-x}Zn_xGeAs_2$:Mn, $ZnSiAs_2$:Mn bulk crystals and to establish correlation among their structural and magnetic properties.

2. EXPERIMENTAL DETAILS

The most probable quasi-binary sections in which $A^{II}B^{IV}C^{V}_2$ compounds can form are the A^{II} - $B^{IV}C^{V}_2$, $A^{II}_3C^{V}_2$-$B^{IV}C^{V}$, and B^{IV}-$A^{II}C^{V}_2$ sections (Fig. 1).[12] The most optimal way to synthesize ternary compound is through the interaction of the components along the B^{IV}-$A^{II}C^{V}_2$ section. The preparation of the batch along this section considerably decreases the free volume in synthetic ampules as compared with the batch consisting of individual components. This ensure the preparation of the stoichiometric composition of the synthesized ternary compound. The preparation of a batch along the A^{II}-$B^{IV}C^{V}_2$ and $A^{II}_3C^{V}_2$-$B^{IV}C^{V}$ sections is less

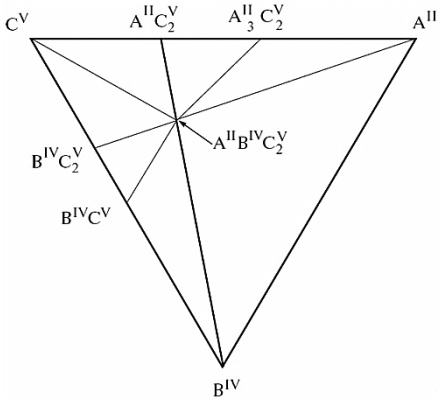

Fig. 1 – Triangulation of the $A^{II}B^{IV}C^{V}_2$ system [12]

* akochura@mail.ru

The article was reported at the International Conference «Physics and Technology of Nanomaterials and Structures», Kursk, 21-22 November, 2013

efficient since the $B^{IV}C^{V}_2$, $A^{II}_3C^{V}_2$, and $B^{IV}C^{V}$ compounds are more difficult to synthesize than the $A^{II}C^{V}_2$ compounds.

To grow of (Zn,Cd)$GeAs_2$ samples, as starting materials was used monocrystalline cadmium and zinc diarsenides prepared by vertical Bridgman technique, high-purity germanium (5N) and manganese (3N). The amounts of the starting materials were controlled by weighing with accuracy of 0.005 %. Because zinc and cadmium diarsenides dissociate upon heating with arsenic vapour evolution, small value of arsenic was added to bathes to adjust stoichiometry. The weight of this additional arsenic was calculated from the arsenic partial vapour pressure of $ZnAs_2$ and $CdAs_2$ and the volume of the ampoule in which the synthesis was carried out. The components were prepared as powders with average particle sizes of 5-10 μm. Total mass of batches placed into quartz ampoules was 9-10 g. The ampoules were evacuated to $1 \cdot 10^{-2}$ Pa and sealed. The synthesis temperature was 1175 K (close to $T_m = 1148$ K of $ZnGeAs_2$) and the synthesis duration was 36 h. To provide maximal solubility of manganese the cooling rate was 10-12 K/s (Fig. 2). Prepared samples of $Zn_{0.9}Cd_{0.1}GeAs_2$ contained 0; 1.13; and 2.65 mas. % of Mn and labeled as #B1, #B2, and #B3, respectively.

The procedure to prepare of Mn-doped $CdGeAs_2$ was like described above for the $Zn_{0.9}Cd_{0.1}GeAs_2$: Mn. The synthesis temperature was 950 K (close to $T_m = 940$ K of $CdGeAs_2$). Prepared samples of $CdGeAs_2$ contained 0.25; 1; and 6 wt % of Mn and labeled as #C1, #C2 and #C3, respectively.

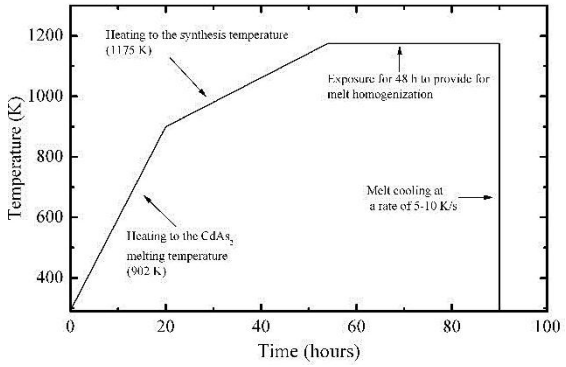

Fig. 2 – Temperature during the synthesis of manganese-doped $Zn_{0.9}Cd_{0.1}GeAs_2$

Specimens of $ZnSiAs_2$:Mn with various Mn concentrations were synthesized by direct melting of high-purity Si, $ZnAs_2$ and Mn powders at a temperature of 10 to 15 K above the $ZnSiAs_2$ melting point (1369 K). The reaction $ZnAs_2 + Si = ZnSiAs_2$ versus time mode is shown in Fig. 2b. This method was developed by analyzing the Zn-Si-As ternary system and its quasibinary sections from Ref. [13]. The synthesis of $ZnSiAs_2$ by $SiAs_2$-Zn section was complicated by high temperature and peritectic nature of $SiAs_2$ melting. If one uses the direct melting of Zn, Si, and As in synthesis, it is difficult to retain stoichiometry because of highly volatile arsenic. The synthesis by $ZnAs_2$-Si section is most suitable because of congruent $ZnAs_2$ melting and low pressure of As vapor. These section was used earler to growth $ZnSiAs_2$:Mn / Si geterostructures [14, 15]. Three polycrystalline $ZnSiAs_2$ samples doped with 0, 1 and 2 wt % Mn, labeled as #E1, #E2 and #E3, respectively, were produced.

Samples structure was investigate by SmartSPM 1000 (AIST-NT Co) scanning probe microscope in AFM mode. The dc magnetization, M, was investigated with a superconducting quantum interference device (SQUID) magnetometer (model S600, Cryogenics ltd.). The measurements were performed separately between 3-310 K and 260 K-580 K in fields up to $B = 5$ T. The dependence of $M(T)$ was measured in B between 5 G and 500 G after cooling the samples from 300 K to 3-5 K in zero field ($B < 0.1$ G) or in the field of the measurements, yielding the data in the zero-field cooled (M_{ZFC}) and the field-cooled (M_{FC}) regimes, respectively.

3. RESULTS AND DISCUSSION

A granular structure was observed in II-IV-As_2:Mn compounds. For example it can be seen for Mn-doped $CdGeAs_2$ (Fig. 3). The mainly part of grains have size from 10 nm up to 150 nm.

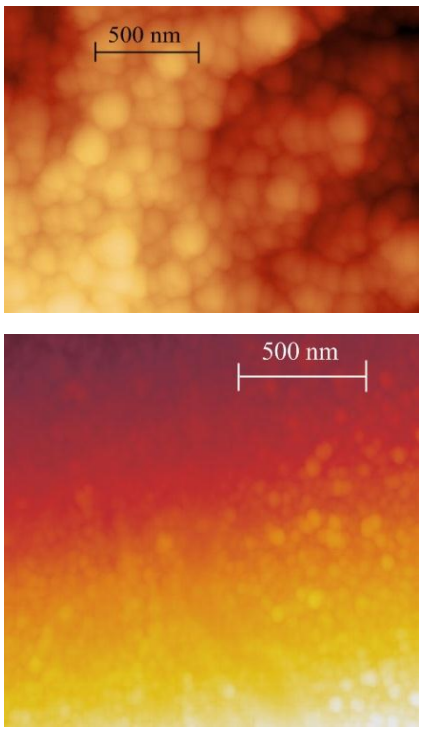

Fig.3 – AFM images of Mn-doped $CdGeAs_2$ samples #C1 (upper image) and #C3 (down image). Clusters and granular structure of samples is clearly visible

The $M(T)$ dependence for samples is complicated. At $T > 100$-150 K the $M(T)$ shape is characteristic of the ferromagnet with different Curie temperatures (Table 1). At low temperatures is seen a sharp increase of magnetization with decrease of temperature. This can be interpreted as an additional contribution of a paramagnetic phase.

The situations when T_C was decreasing up to 320-330 K with magnetic field decreasing and PM T_C belonged to the same interval were observed for all other Mn-doped $A^{II}B^{IV}C^{V}_2$ samples, exhibiting FM ordering.

Table 1 – Curie temperatures of ferromagnetic Mn-doped $A^{II}B^{IV}C^{V}_2$

Compound	Sample number	T_C, K
$Zn_{0.9}Cd_{0.1}GeAs_2$	#B2	349
	#B3	351
$CdGeAs_2$	#C3	337
$ZnSiAs_2$	#E1	325
	#E2	337

These results give evidence that high-temperature ferromagnetism in our samples originates from MnAs phase.

MnAs is ferromagnetic semimetal. In zero magnetic field $T_C = 306$ K and at $T < T_C$ the MnAs has hexagonal structure [16].

Samples of $A^{II}B^{IV}C^{V}_2$ compounds doped with Mn up to 1% wt were paramagnetic. Fig. 4 demonstrate $M(T)$ curves for single crystal $CdGeAs_2$ doped with Mn 0.89 wt % (sample #D2) and 0.006 wt % (sample #D1). For sample #D2 $M(T)$ obeys the Langeven function $M = M_0\left[\coth(\mu B/k_BT) - k_BT/\mu B\right]$ with the mean magnetic moment of clusters $\mu = 7.1\ \mu_B$ and a specific magnetization $M_0 = 1.1$ emu/g. For polycrystalline sample #C2 these values were $\mu = 6.6\ \mu_B$ and $M_0 = 1.3$ emu/g. It is in good agreement with results of Ref. 17 when $\mu = 7.1$-$8.0\ \mu_B$ was obtained for $CdGeAs_2$ doped with Mn from 0.5 up to 6 wt %. The magnetic moment of uncoupled Mn^{2+} ion is $\mu(Mn^{2+}) = 5\ \mu_B$.

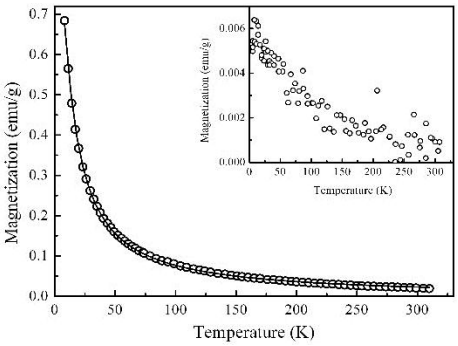

Fig. 4 – The temperature dependence of magnetization $M(T)$ of sample #E2 in 50 kG. The continuous line represent the Langeven function with fitting parameter giving in the text. Inset: The temperature dependence of magnetization of sample #E1 in 50 kG

The value of magnetic moment ≈ 7 μ_B is bigger than is $\mu(Mn^{2+})$. Theoretical calculations performed for (Ga, Mn)As system showed the possibility of Mn clustering into stable and electronically active dimmer, trimmer or tetramer [18]. In these complexes Mn atoms placed on the positions in neighbor unit cells and interact antiferromagnetically. Therefore their effective magnetic moment is reduced. Mn atoms from complexes interact with other type atoms too, especially with As. So the most probably value of μ for Mn atoms is close to $\mu(MnAs) \approx 3.4\ \mu_B$ [19].The value of magnetic moment ≈ 7 μ_B is support of the assumption that most of Mn atoms in lattice formed dimmers.

Presence of nanosize MnV precipitations was observed by magnetic measurements at low magnetic fields. Typical $M(T)$ dependences of $A^{II}B^{IV}C^{V}_2$:Mn measured in ZFC and FC regimes are shown in Fig. 5.

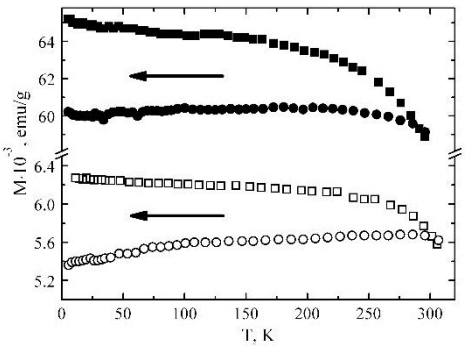

Fig. 5 – Temperature dependences of magnetization, measured in low magnetic fields: M_{ZFC} (circles) and M_{FC} (squares) for $Zn_{0.9}Cd_{0.1}GeAs_2$:Mn sample #B2 at $B = 5$ G (open symbols), (solid symbols) at $B = 50$ G

The magnetic properties of $A^{II}B^{IV}C^{V}_2$:Mn are determined mostly by small ferromagnetic MnAs particles. When T is more or above the blocking temperature the thermal fluctuations lead to that assembly of such clusters exhibit superparamagnetic behavior [20].

The moment of each particle is stabilized independently when anisotropy energy KV (K is the density of the anisotropy energy, V is the average volume of the particles), becomes enough to counteract the thermal excitations about k_BT. After removal of the external field the moments of the particles relax towards equilibrium state. When the relaxation time with value 10^2 s is used as the criterion for transition to stable state the energy barrier must be $25\ k_BT$. Then the blocking temperature of FM particles is [21]

$$T_b = \frac{KV}{25k_B} \tag{1}$$

The susceptibility of a system of arbitrary clusters can be written in the form [20]:

$$\chi_{ZFC}(T) = \chi_0 + \frac{C}{T}\int_0^T f(T_1)dT_1 \tag{2}$$

where χ_0 is χ_{ZFC} at $T < T_b$, C is Curie constant for clusters and $f(T)$ is the distribution function of the blocking temperatures. Using of the small magnetic field during measurements is required to avoid the influence of stable ferromagnetic (nonsuperparamagnetic) clusters on the susceptibility. The low-field contribution to χ from such kind of clusters is small and depends on T only by σ_s. So the first term in eq. 2 represent the contribution of stable clusters and the second term correspond to contribution of superparamagnetic clusters. Parameters χ_0 and C depends only on σ_s and can be express as $\gamma\alpha\sigma_s$ and $\gamma\sigma_s$, respectively (α and γ are constants). Then eq.2 can be written as [20]

$$\chi_{ZFC}(T) = \gamma\sigma_s^2\left(\alpha + \frac{1}{T}\int_0^T f(T_1)dT_1\right) \tag{3}$$

After differentiation of eq. 3 with respect to T the $f(T)$ can be found as [20]

$$f(T) = \frac{1}{\gamma}\frac{d}{dT}\left(\frac{\chi_{ZFC}T}{\sigma_s^2}\right) - \alpha \tag{4}$$

Using of this expression together with eq. 1 let to calculate in a numerical form the distribution function $f(R)$ of the radius of the sphere corresponding to the cluster volume $V = 4\pi r^3/3$. The basic plots of temperature dependences of K and σ_s for MnAs were taken from the ref. 21 and used in interpolation with a rational beta-spline function. Low temperature parts of $K(T)$ and $\sigma_s(T)$ were found by linear extrapolation. The constants λ and γ are determined by normalizing $f(r)$ to unity and using the condition $f(r) = 0$ at $r = 0$. Fitting $f(R)$ with Gaussian function:

$$f(r) = \frac{1}{\sqrt{2\pi}} e^{-\frac{(r-\bar{r})}{2\delta^2}} \quad (5)$$

gives the most probable radius of clusters $\bar{r}$ and mean-square deviation δ (Table 2). The clusters magnetic moment μ (Table 2) calculated with expression $\mu = \mu_{300\,K}\, V/v$ where the volume v and magnetic moment $\mu_{300\,K}$ per MnAs pair are $v \approx 34$ Å^3 [22] and $\mu_{300\,K} \approx 2.3\ \mu_B$ [23], respectively. Our values of μ agree with results of Ref. 24 where $\mu = (1.2\text{-}2.0)\cdot 10^4$ was obtained for Mn-doped $ZnSiAs_2$ without clear explanation about the nature of magnetic clusters. The mean cluster radius increase when increase Mn content. At low Mn concentrations (sample #E2) $f(R)$ has more complex character and described by sum of two Gaussian functions. The same situation was observed in Ref. 20 for $Zn_{1-x}Mn_xAs_2$.

Table 2 – Parameters of MnAs nanoclusters in different II-VI-As2:Mn samples

Sample	$\bar{r}$, nm	δ, nm	μ(300 K), μ_B
#B2	3.7	1.0	$1.4\cdot 10^4$
#B3	3.8	1.1	$1.6\cdot 10^4$
#E2	2.76	0.72	$6.0\cdot 10^3$
	3.10	0.35	$8.5\cdot 10^4$
#E3	3.57	0.96	$1.3\cdot 10^4$

4. CONCLUSION

In summary, we have investigated the structural and magnetic properties of bulk polycrystalline $A^{II}B^{IV}C^{V}_2$ semiconductors with different Mn contents. We have observed their nanocrystalline structure with grains size ranged from 10 nm up to 150 nm. Curie temperatures of ferromagnetic Mn-doped $A^{II}B^{IV}C^{V}_2$ were in the interval 325-351 K. The high temperature ferromagnetic properties were formed by MnAs clusters with mean diameter above 3 nm. Some influence of Mn complexes was observed.

ACKNOWLEDGMENTS

This work was supported by Ministry of Education and Science of the Russian Federation with Grant No. 3.5536.2011.

REFERENCES

1. V.A. Ivanov, T.G. Aminov, V.M. Novotortsev and V.T. Kalinnikov, *Russian Chemical Bulletin* **53**, 2357 (2004).
2. T. Jungwirth, J. Sinova, J. Maŝek, J. Kuĉera J, A.H. MacDonald, *Rev. Modern. Phys.* **78**, 809 (2006).
3. M. Sawicki, D. Chiba, A. Korbecka, Y. Nishitani, J.A. Majewski, F. Matsukura, T. Dietl, H. Ohno, *Nat. Phys.* **6**, 22 (2010).
4. K. Olejnik, M.H.S. Owen, V. Novak, J. Maŝek, A.C. Irvine, J. Wunderlich, T. Jungwirth, *Phys. Rev. B* **78**, 054403 (2008).
5. L. Chen, X. Yang, F. Yang, J. Zhao, J. Misuraca, P. Xiong, and S. von Molnar, *Nano Lett.* **11**, 2584 (2011).
6. *A^{II} – B^{IV} – C Semiconductors*, Ed by N.A. Goryunova, Yu. A. Rud', and Yu. A. Valov (Sov. Radio, Moscow, 1974).
7. G.A. Medvedkin, *Technical Phys. Lett.* **28**, 889 (2002).
8. S.C. Erwin, I. Zutic, *Nat. Mater.* **3**, 410 (2004).
9. K. Sato, G.A. Medvedkin, T. Nishi, Y. Hasegawa, R. Misawa, K. Hirose, T. Ishibashi, *J. Appl. Phys.* **89**, 7027 (2001).
10. V.M. Novotortsev, A.V. Kochura, and S.F. Marenkin, *Inorg. Mater.* **46**, 1421 (2010).
11. L.I. Koroleva, V.Yu. Pavlov, D.M. Zashchirinskiĭ, S.F. Marenkin, R. Szymczak, S.A. Varnavsky, W. Dobrowolski, L. Kilanski, *Phys. Solid State* **49**, 2121 (2007)
12. V.M. Novotortsev, S.F. Marenkin, I.V. Fedorchenko, and A.V. Kochura, *Russ. J. Inorg. Chem.* **55**, 1762 (2010).
13. I.V. Fedorchenko, T.A. Kupriyanova, S.F. Marenkin, A.V. Kochura, *Russ. J. Inorg. Chem.* **53**, 1139 (2008).
14. A. Kochura, I. Fedorchenko, R. Laiho, A. Lashkul, E. Lahderanta, S. Marenkin and I. Zakharov. *phys. status solidi (c)* **6**, 1336 (2009).
15. I.V. Fedorchenko, A.V. Kochura, S.F. Marenkin, A.N. Aronov, L.I. Koroleva, L. Kilanski, R. Szymczak, W. Dobrowolski, S. Ivanenko, and E. Lahderanta. *IEEE T. Magn.* **48**, 1581 (2012).
16. L. Pultik, and A. Zieba, *J. Magn. Magn. Mater.* **51**, 199 (1985).
17. V.M. Novotortsev, V.T. Kalinnikov, L.I. Koroleva, R.V. Demin, S.F. Marenkin, T.G. Aminov, G.G. Shabunina, S.V. Boijchuk, and V.A. Ivanov. *Russ. J. Inorg. Chem.* **50**, 492 (2005).
18. H. Raebiger, A. Ayuela, J. von Boehm, *Phys. Rev. B* **72**, 014465 (2005).
19. S. Sanvito, N.A. Hill, *Phys. Rev. B* **62**, 15553 (2000).
20. R. Laiho, K.G. Lisunov, E. Lahderanta V.S. Zakhvalinskii, *J. Phys. Cond. Matter.* **11**, 555 (1999).
21. C.P. Bean, J.D. Livingstone, *J. Appl. Phys.* **30**, S120 (1959).
22. R.W. De Blois, D.S. Rodbell, *J. Appl. Phys.* **34**, 1101 (1963).
23. N. Menyuk, J.A. Kafalas, K. Dwight, J.B. Goodenough, *Phys. Rev.* **177**, 942 (1969).
24. L.I. Koroleva, D.M. Zashirinskii, T.M. Khapaeva, S.F. Marenkin, I.V. Fedorchenko, R. Szymczak, B. Krzumanska, V. Dobrovolskii, L. Kilanskii, *Phys. Solid State* **51**, 303 (2009).